HHS Public Access

Author manuscript

J Neurosci Res. Author manuscript; available in PMC 2022 June 02.

Published in final edited form as:

J Neurosci Res. 2011 July ; 89(7): 1001–1017. doi:10.1002/jnr.22624.

Spatial and Temporal Changes in Promoter Activity of the Astrocyte Glutamate Transporter GLT1 Following Traumatic Spinal Cord Injury

Angelo C. Lepore[1], **John O'Donnell**[1], **Joseph F. Bonner**[2], **Courtney Paul**[2], **Mark E. Miller**[2], **Britta Rauck**[1], **Robert A. Kushner**[2], **Jeffrey D. Rothstein**[1], **Itzhak Fischer**[2], **Nicholas J. Maragakis**[1,*]

[1]Department of Neurology, The Johns Hopkins University School of Medicine, Baltimore, Maryland

[2]Department of Neurobiology and Anatomy, Drexel University College of Medicine, Philadelphia, Pennsylvania

Abstract

After traumatic spinal cord injury (SCI), there is an opportunity for preserving function by attenuating secondary cell loss. Astrocytes play crucial roles in the adult CNS and are responsible for the vast majority of glutamate buffering, potentially preventing excitotoxic loss of neurons and oligodendrocytes. We examined spatial and temporal changes in gene expression of the major astrocyte glutamate transporter GLT1 following moderate thoracic contusion SCI using transgenic BAC-GLT1-eGFP promoter reporter mice. In dorsal column white matter, total intensity of GLT1-eGFP expression per region was significantly reduced following SCI at both lesion epicenter and at rostral and caudal areas where no tissue loss occurred. This regional decrease in GLT1 expression was due to significant loss of GLT1-eGFP$^+$ cells, partially accounted for by apoptosis of eGFP$^+$/GFAP$^+$ astrocytes in both white and gray matter. There were also decreased numbers of GLT1-eGFP-expressing cells in multiple gray matter regions following injury; nevertheless, there was sustained or even increased regional GLT1-eGFP expression in gray matter as a result of up-regulation in astrocytes that continued to express GLT1-eGFP. Although there were increased numbers of GFAP$^+$ cells both at the lesion site and in surrounding intact spinal cord following SCI, the majority of proliferating Ki67$^+$/GFAP$^+$ astrocytes did not express GLT1-eGFP. These findings demonstrate that spatial and temporal alterations in GLT1 expression observed after SCI result from both astrocyte death and gene expression changes in surviving astrocytes. Results also suggest that following SCI a significant portion of astrocytes lacks GLT1 expression, possibly compromising the important role of astrocytes in glutamate homeostasis.

Keywords

secondary injury; BAC reporter mice; contusion; glutamate uptake; excitotoxicity

[*]Correspondence to: Nicholas J. Maragakis, MD, Department of Neurology, The Johns Hopkins School of Medicine, John G. Rangos Bldg., 855 N. Wolfe St., Rm. 248, Baltimore, MD 21205. nmaragak@jhmi.edu.

Traumatic spinal cord injury (SCI) has debilitating consequences that depend on level and severity of injury (McDonald and Becker, 2003). Initial injury results in cell death and axotomy of passing fibers. Acute stages are followed by a period of secondary cell death that produces additional functional deficits (Norenberg et al., 2004). Most human SCI cases do not produce complete transection; therefore, an opportunity exists for preserving function via attenuation of secondary degeneration (Baptiste and Fehlings, 2006).

Glutamate-mediated cell death plays a key role in secondary events following traumatic CNS injuries such as SCI (Park et al., 2004; Stys, 2004; Yi and Hazell, 2006). Parenchymal administration of glutamate to normal spinal cord results in tissue and functional loss similar to that of SCI (Xu et al., 2005). Large increases in extracellular excitatory amino acids such as glutamate occur after SCI as well (Liu et al., 1991; Xu et al., 2004). Up to 50-fold increases in extracellular glutamate can occur shortly following SCI (Panter et al., 1990), and elevated levels can persist for over 1 week and appear to vary with injury severity. In addition to focal increases, glutamate levels can rise in regions removed from the lesion site, possibly via a spreading mechanism involving activated glia (Hulsebosch, 2008).

Early gray matter cell loss likely is mediated by N-methyl-D-aspartate (NMDA) receptors, whereas delayed loss of gray matter neurons and white matter oligodendrocytes and axonal injury are thought to be mediated predominantly via AMPA overactivation (Stys, 2004). The role of specific receptors is based on selective expression of glutamate receptor subtypes by different cell populations (Park et al., 2004). Changes in glutamate receptor subunit composition following SCI, as well as events such as posttranslational modification of receptor subunits, can alter receptor properties, thereby modifying their response to glutamate elevation (Grossman et al., 1999, 2000; Mills et al., 2001; Park et al., 2003). The NMDA receptor antagonist MK-801 showed mixed results in various SCI paradigms, producing efficacy in only some studies (Holtz and Gerdin, 1991; Liu et al., 1997; Agrawal and Fehlings, 1997; Gaviria et al., 2000). The AMPA receptor antagonist NBQX, promoted both gray and white matter tissue sparing, bladder function improvement, and decreases in allodynia and hyperalgesia in a number of studies (Wrathall et al., 1994; Agrawal and Fehlings, 1997; Liu et al., 1997; Rosenberg et al., 1999; Mu et al., 2002). These receptor-acting drugs have shown promise, but they also result in unwanted side effects. It may be advantageous to address glutamate toxicity focally by targeting the normal physiological function of astrocytes, those cells that normally play the central role in regulating CNS glutamate homeostasis.

Astrocytes outnumber their neuronal counterparts by approximately tenfold and play many crucial roles in adult CNS function, including the vast majority of CNS glutamate uptake (Tanaka et al., 1997). The two major CNS glutamate transporters, GLT1 and GLAST, are expressed almost exclusively by astrocytes in the adult (Maragakis and Rothstein, 2004). GLT1 expression levels are highest in gray matter regions of the spinal cord, with less expression observed in white matter areas. GLAST is thought to be expressed by most astrocytes throughout the spinal cord; nevertheless, overall expression and functional glutamate uptake is significantly greater for GLT1 than for GLAST in most CNS regions (Danbolt, 2001). After SCI, astrocytes hypertrophy and interdigitate to form a dense reactive astroglia scar. Astrocyte death, altered physiology of astrocytes and their transporters, and/or

changes in expression of key astrocyte proteins such as glutamate transporters may result in further susceptibility to excitotoxic death of neurons and oligodendrocytes, thereby contributing to secondary injury. Few studies have examined the role of astrocyte glutamate transport following SCI. This study was aimed at elucidating temporal and spatial changes in gene expression of the major astrocyte glutamate transporter, GLT1, following SCI. Results will provide valuable information both for understanding the role that astrocyte glutamate transport plays in the host response to SCI and for designing therapeutic strategies targeting the physiological function of astrocytes.

MATERIALS AND METHODS

Transgenic BAC-GLT1-eGFP Promoter Reporter Mice

Transgenic BAC (bacterial artificial chromosome)-GLT1-eGFP promoter reporter mice allow for the examination of GLT1 promoter activity in regions throughout the CNS. GLT1 promoter activity drives expression of the eGFP reporter. The BAC construct contains the entire 123-kb GLT1 gene, in addition to 45 kb upstream of the first exon and 24 kb downstream of the last exon. In addition, the eGFP coding sequence was inserted downstream of the GLT-1 promoter, between the AT and the G of the start codon (Regan et al., 2007).

Contusion Injury

The care and treatment of animals in all procedures was conducted in strict accordance with the guidelines set by the European Communities Counsel Directive (November 24, 1986), the NIH *Guide for the care and use of laboratory animals*, the *Guidelines for the use of animals in neuroscience research*, and the Johns Hopkins University IACUC and the Drexel University IACUC, and measures were taken to minimize any potential pain or animal discomfort. Mice weighing approximately 20–30 g received i.p. injections of anesthetic cocktail [acepromazine maleate (0.7 mg/kg; Fermenta Animal Health, Kansas City, MO), ketamine (95.0 mg/kg; Fort Dodge Animal Health, Fort Dodge, IA), and xylazine (10.0 mg/kg; Bayer, Shawnee Mission, KS)]. The back musculature was excised and a laminectomy was performed above the T8–T10 levels of the spinal cord. Adult nontransgenic (Jackson, Bar Harbor, ME) and BAC-GLT1-eGFP promoter reporter mice received a moderate thoracic (T9) contusion SCI using the IH impactor, as described previously (Basso et al., 2006). Control animals underwent the same surgery, including laminectomy, but did not receive contusion injury. After surgical procedures, animals were allowed to recover on a circulating warm water heating pad until awake and then returned to their home cages, usually requiring a continuous observations period of 2–4 hr. Animals were monitored on a daily basis thereafter. Antibiotic powder was applied to the closed wounds to prevent infection. Bladders were expressed twice daily during the first week following injury.

Tissue Processing

Euthanasia was performed by inhalation anesthesia to minimize pain and distress. This method is consistent with the recommendations of the Panel on Euthanasia of the American Veterinary Medical Association. Both control and contusion mice were sacrificed at 1, 4,

and 14 days postinjury by transcardial perfusion with 0.3% saline, followed by ice-cold 4% paraformaldehyde (Fisher Scientific, Pittsburgh, PA). The entire spinal cord was removed, and the thoracic region was isolated and postfixed in 4.0% paraformaldehyde, followed by cryprotection in 30% sucrose (Fisher Scientific)/0.1 M phosphate buffer at 4°C for 3 days. Tissue surrounding the lesion site was embedded in OCT (Fisher Scientific), fast frozen with dry ice, and stored at −80°C until processed. Spinal cord tissue blocks were cut serially in the transverse plane at 20 μm thickness. Sections were collected on glass slides and stored at −20°C until analyzed.

Histological Analysis

Cresyl violet staining and lesion identification. -—Sections were stained with cresyl violet and imaged (Paul et al., 2009). The lesion epicenter region was defined as sections in which clear tissue destruction was present, and rostral and caudal regions were defined as sections within 1 mm of the rostral or caudal edges of the epicenter, respectively, in which no visible tissue destruction was present.

Analysis of BAC-GLT1-eGFP expression.—For quantitative analysis of BAC-GLT1-eGFP fluorescence, a one-in-five series of serially sectioned slides was washed in 1× TBS, counterstained with DAPI, and coverslipped with Fluorosave, and then fluorescence was imaged with a ×10 objective from sections throughout the extent of the spinal cord (rostral intact cord, lesion site, caudal intact cord). From each transverse section, images of eGFP from dorsal column white matter, dorsal horn gray matter, ventral horn gray matter, and intermediate gray matter were acquired using the exact same camera settings for all sections, and images were not further modified. eGFP fluorescence (which serves as a marker of GLT1 expression within the spinal cord) was quantified in a number of ways. Transverse sections of spinal cord were divided into three segments in the rostral–caudal orientation as described above: epicenter, rostral, and caudal regions. Within the three areas, sections were further subdivided into regions: dorsal column white matter, dorsal horn gray matter, intermediate gray matter, and ventral horn gray matter. With Metamorph software, each individual GLT1-eGFP$^+$ cell was identified, and the regions of eGFP fluorescence for all eGFP$^+$ cells were outlined. To analyze the eGFP fluorescence signal, the 1) area and 2) intensity of each eGFP$^+$ cell within a region were analyzed (in Metamorph). The collective data from all cells within a region were then expressed as 1) GLT1-eGFP area/cell (defined as cell expressing eGFP), 2) GLT1-eGFP intensity/cell, 3) total GLT1-eGFP intensity of all cells in a region (sum of the intensity of all individual eGFP-expressing cells in a region), and 4) total numbers of eGFP$^+$ cells per region. This extensive system of analysis allowed for specific examination of changes both temporally and spatially following SCI. eGFP expression was analyzed both on an individual cell basis and on a regional basis to determine the response of individual astrocytes following SCI as well as the larger regional changes occurring in specific locations.

Immunohistochemistry.—To assess the phenotype of eGFP$^+$ GLT1-expressing cells, sections were immunolabeled with markers (Lepore et al., 2004, 2005, 2006a,b, 2008a,b; Lepore and Fischer, 2005; Mitsui et al., 2005) of neurons (NeuN), astrocytes (GFAP), and oligodendrocytes (RIP; Watanabe et al., 2006). Double staining for the proliferation marker

Ki67 with GFAP was used to identify and quantify the populations of dividing astrocytes within the spinal cord. Cleaved caspase-3 was used to identify astrocytes undergoing apoptosis. Samples were incubated for 2 hr at room temperature with goat anti-mouse and goat anti-rabbit secondary antibodies (1:200, Jackson Immunoresearch, West Grove, PA; 1:1,000, Molecular Probes, Eugene, OR) conjugated to rhodamine, FITC, or Alexa Fluor 633. Samples were counterstained with DAPI (1:1,000; Sigma, St. Louis, MO) to identify nuclei and coverslipped with antifade mounting media (Fluorosave; CN Biosciences, La Jolla, CA). Apoptotic cells were also identified using the Promega Dead End TUNEL System (Promega, Madison, WI) combined with streptavidin conjugated to Alexa Fluor 555 (1:500; Molecular Probes). Controls in which the primary antibody (for GFAP, Ki67, cleaved capsase-3) or biotinylated nucleotide (for TUNEL) was omitted were used, and all immunostainings were found to be specific (Fig. 7C). Slides were subsequently stored at 4°C. Images were acquired on either a Zeiss fluorescence microscope using a Photometric Sensys KAF-1400 CCD camera (Roper Scientific; Trenton, NJ) or a Zeiss laser confocal microscope. Images were analyzed in either Metamorph or Zeiss confocal software. Adobe Photoshop CS (Adobe, San Jose, CA) was used to prepare figures.

Antibody Characterization

GFAP (Dako, Carpinteria, CA; No. Z0334; rabbit polyclonal; 1:400) was raised against cow spinal cord and recognizes astrocytes throughout the white and gray matter of the intact and injured CNS (Lepore et al., 2008a). Using crossed immunoelectrophoresis and indirect ELISA, antibody reactivity was not seen with human plasma or cow serum. On immunocytochemistry, the antibody reacts with cat, dog, mouse, rat, sheep, human, and cow GFAP (according to the manufacturer's technical information). A second GFAP antibody (Millipore, Bedford, MA; MAB360; clone GA5; mouse monoclonal; 1:200) was raised against purified GFAP form porcine spinal cord. The antibody recognizes a 51-kDa band corresponding to GFAP via Western blotting of human glioma cell line extract and also labels astrocytes via immunohistochemistry (according to the manufacturer's technical information). NeuN (Millipore; MAB377; clone A60; mouse monoclonal: 1:100) was raised against purified cell nuclei from mouse brain and reacts with most neuronal cell types throughout the mouse CNS and PNS (Lepore and Fischer, 2005). RIP (Millipore; MAB1580; antioligodendrocytes, clone NS-1; mouse monoclonal; 1:3,000) was raised against rat olfactory bulb and recognizes both early and mature oligodendrocytes and myelin sheaths (Lepore et al., 2004). Ki67 (Thermo, Fair Lawn, NJ; No. RM-9106-S; clone SP6; rabbit monoclonal; 1:400) was raised against a synthetic peptide derived from human Ki67 protein (C-terminus) and recognizes all proliferating cells, regardless of lineage (Lepore et al., 2008a). Cleaved capsase-3 (Cell Signaling Technology, Beverly, MA; No. 9664; Asp175/5A1; rabbit monoclonal; 1:100) was raised against a synthetic peptide corresponding to amino terminal residues adjacent to Asp175 of human caspase-3 and recognizes cells undergoing apoptosis. On Western blotting, the antibody detects the endogenous large fragment of activated caspase-3 adjacent to residue Asp 175 but does not recognize full-length caspase-3 or other caspases (according to the manufacturer's technical information). Refer to Table I for summary information of all antibodies used in this study.

Statistical Analysis

BAC-GLT1-eGFP data were analyzed via ANOVA using the statistical software Sigmastat (SAS Software). In some cases, Student's *t*-test was performed to compare data between groups. All data are presented as mean ± SEM, and the significance level was set at $P \leq 0.05$.

RESULTS

Analysis of Thoracic Contusion SCI in Mice

Cresyl violet-stained sections of thoracic spinal cord from mice that had received a moderate contusion (T9) show the changing lesion composition while moving caudally throughout the injury site. Distinct differences can be observed among intact spinal cord immediately rostral to the injury site (Fig. 1A), the rostral periphery of the lesion site (Fig. 1B), and the center of the injury (Fig. 1C). For BAC-GLT1-eGFP analysis, cresyl violet staining was used to determine the sections in which tissue loss occurred. At the most severe sections of the epicenter, most of the structure of both gray and white matter was lost. Moving away from the epicenter both rostrally and caudally, the injury resulted in decreasing levels of tissue loss, with the lesion being most pronounced in the dorsal column and dorsal horns. For analysis, spinal cord cross-sections were first subdivided into specific anatomical locations (Fig. 1D): dorsal column white matter (DC), dorsal horn gray matter (DH), intermediate gray matter (Int), and ventral horn gray matter (VH).

Analysis of Transgenic GLT1-eGFP Mice After Thoracic Contusion SCI

Characterization of transgenic BAC-GLT1-eGFP promoter reporter mice has been previously reported (Gincel et al., 2007; Regan et al., 2007). GLT1 promoter activity drives expression of the eGFP reporter (Fig. 1E), allowing for spatial and temporal examination of astrocyte glutamate transporter promoter activity following SCI. In normal, uninjured animals (Fig. 1E–G), GLT1 is found in abundance in gray matter and to a lesser extent in white matter. To analyze GLT1-eGFP promoter activity in astrocytes in uninjured spinal cord and following SCI (rostral intact cord: Fig. 1H; epicenter: Fig. 1I), individual $eGFP^+$ cells were identified within each of the locations outlined in Figure 1D, and the region of fluorescence for each $eGFP^+$ cell was outlined. The eGFP intensity and area for each $eGFP^+$ cell were measured in Metamorph software (Fig. 1J).

Quantification of Changes in GLT1 Promoter Activity After Thoracic Spinal Cord Contusion

BAC-GLT1-eGFP promoter reporter mice received a moderate thoracic (T9) contusion and were sacrificed at 1, 4, and 14 days post-SCI. Uninjured control animals received a laminectomy without contusion and were also sacrificed at the same three time points (n = 6/time point: three control and three injured) following surgery as SCI mice in order to obtain the appropriate controls. Analysis of eGFP fluorescence in uninjured control mice at 1, 4, and 14 days showed that there were no significant differences in eGFP expression within a given region among the three time points ($*P > 0.05$; data not shown); therefore, control mice data from all three time points were combined. Refer to Materials and Methods for a detailed description of eGFP analysis.

White matter.—Quantification of eGFP expression changes following contusion injury in the dorsal column white matter (Fig. 1D) demonstrates that there were no significant alterations in the intensity (Fig. 2A) or area (Fig. 2B) of eGFP expression per cell (defined as cell expressing eGFP) in regions either rostral or caudal to the injury site, with the exception of rostral regions at 4 days. The intensity per cell was reduced at the epicenter at all three time points, and the area per cell was increased at the epicenter at 4 and 14 days. This suggests that astrocytes in white matter lesion regions hypertrophy and down-regulate GLT1 expression.

The total intensity (Fig. 2C) of eGFP fluorescence per region (sum of the intensity of all individual eGFP-expressing cells in a region) was reduced at one or more time points at rostral, epicenter and caudal areas following injury. These changes were most dramatic at the epicenter, and could be expected because of the loss of tissue. Interestingly, significant losses of total regional eGFP expression intensity were also noted in rostral and caudal areas, where no gross tissue loss occurred. The loss of total eGFP expression per region was due to decreased total numbers of $eGFP^+$ cells in all areas, with the most significant losses occurring at the epicenter of the injury (Fig. 2D). In the caudal area, the numbers of $eGFP^+$ cells had returned to control levels by 14 days, after the time when the majority of secondary degeneration likely has occurred.

Gray matter.—Gray matter was subdivided into dorsal horn, intermediate area, and ventral horn for analyses, as illustrated in Figure 1D. There were significant increases in GLT1-eGFP fluorescence intensity (Fig. 3A) and area (Fig. 3B) per cell at multiple time points following injury in all gray matter regions examined. Unlike the case in dorsal column white matter, regional GLT1-$eGFP^+$ cell intensities (sum of individual cell intensities of all GLT1-$eGFP^+$ cells in region; Fig. 4A) were comparable to or greater than controls in all regions, except in those regions that suffered the greatest cell loss, the rostral dorsal horn and the lesion epicenter at dorsal, intermediate, and ventral gray matter regions. Increased regional GLT1-eGFP expression likely was due to the increases observed in GLT1-eGFP intensity per cell (Fig. 3A). Similarly to dorsal column white matter, counts of total numbers of $eGFP^+$ cells showed decreases across most gray matter locations and time points (Fig. 4B). Although the greatest losses were predictably located at the epicenter of the lesion, significant losses of $eGFP^+$ cell numbers were also observed at locations both rostral and caudal to the epicenter at multiple time points, where no gross tissue loss was observed. Interestingly, larger cell losses were observed at dorsal, intermediate, and ventral gray matter regions in rostral sections than in caudal sections.

Even with decreased total numbers of cells expressing GLT1-eGFP, regional intensities were still found to be comparable to or greater than controls in most regions. This was most pronounced at the injury epicenter. Despite significant loss in total GFP+ cell numbers, eGFP-expressing astrocytes in the epicenter exhibited the largest increase in both eGFP intensity and eGFP area per cell, with total regional eGFP intensity in the injury epicenter still remaining comparable to uninjured controls. Refer to Table II for a summary of the white and gray matter changes in GLT1-eGFP expression following contusion injury.

Reactive Astrocytes Did Not Show GLT1 Promoter Reporter Activity After SCI

The decreases observed in total numbers of astrocytes expressing eGFP in both white and gray matter regions may be due to actual loss of astrocytes following injury. However, astrogliosis following SCI is well-established, including proliferation leading to increased numbers of $GFAP^+$ cells (Faulkner et al., 2004). To explore the astrocyte response following SCI, double labeling with the astrocyte lineage-specific marker GFAP and the BAC-GLT1-eGFP reporter was used to determine the cell populations with GLT1 promoter activity, and particular notice was paid to regions of astrogliosis surrounding the injury (n = 3/group/region). In uninjured spinal cord, eGFP was expressed only in $GFAP^+$ astrocytes, and nearly all $GFAP^+$ astrocytes expressed eGFP (Fig. 5A,B: gray matter; Fig. 5A, inset: white matter; Fig. 5F,G). $eGFP^+$ cells were also not found to express neuronal (NeuN) or oligodendrocyte (RIP) markers (not shown). At 4 days following SCI, there was a pronounced increase in $GFAP^+$ astrocytes in dorsal column white matter (Fig. 5E), both at the epicenter (Fig. 5C,D) and in intact spinal cord immediately adjacent to the epicenter of the injury. However, there was also an overall decrease in numbers of eGFP-expressing cells (see Figs. 2–4). Although eGFP expression was still restricted to $GFAP^+$ astrocytes following SCI (Fig. 5D,G), a large proportion of the increased numbers of $GFAP^+$ astrocytes found at the injury site and immediate adjacent spinal cord did not express eGFP (Fig. 5C,D: white matter; Fig. 5C, inset: ventral gray matter; Fig. 5E,F).

Astrocytes Proliferated but Did Not Have GLT1 Promoter Activity After SCI

The increased number of astrocytes likely was derived from proliferating $Ki67^+/GFAP^+$ astrocytes that were observed throughout the lesioned spinal cord (Fig. 6A,B). In uninjured spinal cord, few proliferating $Ki67^+$ cells were observed (Fig. 6D). At 4 days following injury, there was a large increase in the numbers of proliferating $Ki67^+$ cells in dorsal column white matter, both at the epicenter and adjacent intact spinal cord (Fig. 6D), and approximately half of the proliferating $Ki67^+$ cells were $GFAP^+$ astrocytes (Fig. 6D,E; n = 3/group/region). The vast majority of proliferating astrocytes did not express eGFP (Fig. 6B–D,F,G), thus explaining why decreased numbers of eGFP-expressing cells were observed following injury despite increased numbers of astrocytes. These findings suggest that, after SCI, astrocytes proliferated but lacked GLT1 promoter activity, unlike quiescent astrocytes in uninjured CNS.

eGFP Expressing Astrocytes Underwent Apoptosis After SCI

To clarify the changes in GLT1 promoter activity following SCI, cell death of astrocytes was examined. Section were triple labeled for the astrocyte marker GFAP, the apoptosis marker cleaved caspase-3, and eGFP (Fig. 7A; n = 3/group/region). At 4 days following injury, thoracic spinal cord sections from BAC-GLT1-eGFP mice were also double labeled with cleaved caspase-3 and the apoptotic marker TUNEL. $eGFP^+$ cells that colocalize with cleaved $caspase\text{-}3^+$ were also $TUNEL^+$ (Fig. 7B), suggesting that $eGFP^+$/cleaved $caspase\text{-}3^+$ astrocytes are in fact undergoing apoptosis. Although positive staining for cleaved caspase-3 might also be indicative of other changes within cells, these findings demonstrate that cleaved caspase-3 immunostaining is an accurate marker of astrocyte apoptosis.

In uninjured spinal cord, there were no apoptotic caspase-3^+ cells observed (Fig. 7D). At 4 days following injury, there was a large increase in the numbers of apoptotic caspase-3^+ cells in dorsal column white matter, both at the epicenter and in adjacent intact spinal cord (Fig. 7D). Approximately 20–30% of the apoptotic caspase-3^+ cells were $GFAP^+$ astrocytes (Fig. 7D,E), suggesting that, although astrocyte apoptosis occurred following SCI, astrocytes were not the major cell type undergoing this form of cell death. $GFAP^+$/$eGFP^+$ astrocytes that were caspase-3^+ were noted both at the epicenter (Fig. 7A) and in adjacent intact spinal cord following SCI, but constituted only a small portion of the apoptotic cells (Fig. 7D,F). Nevertheless, approximately 10–20% of $eGFP^+$ cells at 4 days postinjury in the dorsal column white matter were caspase-3^+ (Fig. 7G), suggesting that apoptosis of $eGFP^+$ cells, though a minor fraction of the total apoptosis occurring in the spinal cord following SCI, played a significant role in the decrease in numbers of GLT1-expressing astrocytes following injury.

Gray Matter Changes in Astrocyte GLT1 Expression, Proliferation, and Apoptosis After SCI

The same set of quantitative analyses shown for dorsal column white matter were also conducted for ventral gray matter using BAC-GLT1-eGFP, GFAP, Ki67, and cleaved caspase-3 markers. Increased numbers of $GFAP^+$ (Fig. 8A) and $Ki67^+$ (Fig. 8D) cells were noted following SCI in both the contusion epicenter and the adjacent intact spinal cord. A large proportion of these additional $GFAP^+$ cells did not express GLT1-eGFP (Fig. 8A,B); however, the percentage of astrocytes expressing GLT1-eGFP in gray matter following injury was greater than that observed in dorsal white matter (Fig. 8B). Many of the dividing $Ki67^+$ cells were $GFAP^+$ astrocytes (Fig. 8D,E); however, the percentage of dividing cells that were $GFAP^+$ astrocytes was reduced compared with dorsal white matter, both at contusion epicenter and in adjacent intact spinal cord. Only a small percentage of dividing $Ki67^+$ cells was GLT1-$eGFP^+$ in gray matter (Fig. 8F,G); however, a greater proportion of GLT1-$eGFP^+$ cells was $Ki67^+$ than in dorsal white matter. Finally, a significant increase in apoptotic cleaved caspase-3^+ cells in gray matter was observed following SCI, both at the contusion epicenter and in adjacent intact spinal cord (Fig. 8H). Compared with white matter, a smaller percentage of apoptotic cells was $GFAP^+$ (Fig. 8I) and GLT1-eGFP-expressing (Fig. 8J,K) astrocytes.

Collectively, these findings demonstrate that the loss of eGFP+ cells observed following SCI in both white and gray matter regions was due partially to death of astrocytes (in addition to some gene down-regulation) and that proliferation of $eGFP^-$ astrocytes did not replace the lost GLT1-expressing astrocytes. Refer to Table III for a summary of GLT1-eGFP expression changes in reactive, proliferating, and dying astrocytes.

DISCUSSION

The present study examined changes in promoter activity of the major astrocyte glutamate transporter, GLT1, following SCI and represents initial characterization of changes that occur in the promoter activity of a critical astrocyte protein. Few studies have examined the role of glutamate transport after traumatic CNS injury. An increase in levels of GLT1 and a second astrocyte glutamate transporter, GLAST, following contusion has been reported

(Vera-Portocarrero et al., 2002); however, expression changes were examined only during the first 24 hr. Glutamate homeostasis continues to be abnormal for long periods of time after SCI (Cao and Zhang, 2008); therefore, it is important to understand the longer-term changes in transporter expression beyond the first day after SCI. Our findings demonstrated that there are specific spatial and temporal alterations in GLT1 promoter activity following SCI. We report a decrease in the total numbers of GLT1-eGFP-expressing cells after SCI in both dorsal column white matter and in multiple gray matter regions, both at the lesion site and in adjacent rostral and caudal intact spinal cord. These changes were associated with decreased total regional expression of GLT1-eGFP in dorsal column white matter, but minimal changes in GLT1-eGFP expression in individual astrocytes. Conversely, loss of total numbers of GLT1-eGFP-expressing cells in the gray matter was associated with sustained, or even increased, total regional GLT1-eGFP expression, which was the result of up-regulation in individual astrocytes. SCI was accompanied by astrogliosis in both white and gray matter regions, including extensive proliferation of astrocytes; however, the vast majority of these new astrocytes did not express GLT1-eGFP. Furthermore, astrocyte apoptosis was noted, particularly of GLT1-eGFP-expressing cells.

A recent study by Olsen et al. (2010) demonstrated a decrease in GLT1 protein expression that persisted for up to 4 weeks in a rat crush model of SCI. Their results coincide with the present findings in that they also observed up-regulation of total GFAP protein accompanying GLT1 expression loss. On the contrary, we examined GLT1 promoter activity changes using BAC reporter mice in a contusion model of SCI. Our study has extended the Olsen et al. findings quantitatively to show loss in total numbers of GLT1-expressing cells in white and gray matter regions as well as differential responses in total GLT1 gene expression in white and gray matter. We have also examined the proliferative and apoptotic response of GLT1-expressing astrocytes in an anatomically specific manner. These complimentary studies point toward changes in GLT1-expressing astrocytes as a significant cellular response to SCI. Future studies are necessary to elucidate the significance of these changes for histopathological and functional outcome following SCI.

What are the mechanisms for the decreased numbers of GLT1-eGFP-expressing astrocytes observed following SCI in both white and gray matter? Death of astrocytes may play a role, especially at the lesion site. Indeed, we observed apoptosis of $GFAP^+$ astrocytes, particularly of GLT1-eGFP-expressing cells, both at the epicenter and in adjacent intact regions. In addition, we found down-regulation of GLT1 expression in populations of surviving GLT1-eGFP astrocytes. This suggests that reduced GLT1 promoter activity in surviving astrocytes also played a major role, in addition to the apoptosis of GLT1-expressing cells observed in intact spinal cord. Previous studies have shown that reduced axonal contact with astrocytes following thoracic transection decreases GLT1 expression in lumbar enlargement astrocytes by affecting GLT1 promoter activity (Yang et al., 2009). After SCI, there was intense astroglial activation, and most of these reactive, proliferating astrocytes did not express GLT1. These findings demonstrate that despite the addition of nascent astrocytes there were still reduced numbers of cells expressing GLT1 because these new, “reactive” astrocytes did not have GLT1 promoter activity. Previous work has demonstrated that reactive astrocytes play an important protective role in early events following SCI (Faulkner et al., 2004). However, lack of GLT1 promoter activity suggests that these cells do not express the full

complement of important astrocyte proteins necessary for CNS homeostasis for at least 2 weeks and may consequently have long-term dysfunctional effects on spinal cord function. Signals expressed following CNS trauma such as increased levels of interleukin-1 can also inhibit the function of GLT1 protein, in addition to effects of injury-related signals on gene and protein expression (Prow and Irani, 2008). We did not measure functional glutamate uptake, because bio-chemical assays of entire host tissues might not account for localized changes within spatially defined regions.

Our findings in the gray matter demonstrate a similar overall pattern in responsiveness of GLT1-expressing, proliferating, and apoptotic astrocytes following contusion injury compared with dorsal column white matter. However, this overall pattern similarity was associated with a number of small, yet interesting, differences in gray matter following SCI, including 1) an increased percentage of $GFAP^+$ cells continuing to express GLT1, 2) an overall decrease in the percentage of proliferating cells that are astrocytes as well as an increase in the percentage of GLT1-expressing cells found to proliferate, and 3) a decrease in the percentage of apoptotic cells that made up of astrocytes as well as a decrease in apoptosis of GLT1-expressing cells. These differences may translate to differential roles for GLT1 at gray vs. white regions following SCI and should be considered when spatially and temporally designing therapeutic strategies targeting GLT1.

Reduced numbers of GLT1-expressing astrocytes following SCI may serve a compensatory role to prevent additional secondary damage. Previous studies using an isolated spinal cord white matter model of ischemic injury demonstrated that glutamate transport inhibition actually decreased oligodendrocyte, myelin, and axonal conduction loss (Li et al., 1999). It was shown that altered transmembrane Na^+ and K^+ gradients caused reversal of transport and extracellular dumping of glutamate. These studies were conducted ex vivo and in an ischemia model and therefore may not reflect the in vivo condition of traumatic SCI.

Although glutamate-mediated cell death is an important contributor to functional loss because of secondary degeneration, elevated glutamate has also been shown to play a key role in neuropathic pain following spinal trauma, which occurs in up to 80% of SCI patients (Tao et al., 2005). The anatomical mechanisms of hyperalgesia, allodynia, and spontaneous pain differ; nevertheless, intense glial activation occurs in all of these types of pain, regardless of whether there is central SCI or peripheral nerve damage (Hansson, 2006). Glutamate has been shown to play a central role in this glial response and may be involved in chronic maintenance of a neuropathic pain state (Hulsebosch, 2008; Hulsebosch et al., 2009).

Overall regional increases in total GLT1 promoter activity were noted at some gray matter areas (but not white matter) and at various time points following SCI. This response may represent compensation for increased levels of extracellular glutamate and/or for the significant decrease in total numbers of astrocytes expressing GLT1 following injury. Even with this increase in gray matter GLT1 expression, excitotoxicity still results in loss of gray matter cells, suggesting that the host response is not sufficient to protect cells against glutamate elevation.

Targeting the actions of glutamate is a promising therapeutic approach insofar as glutamate-mediated secondary injury and neuropathic pain represent a treatment target that is theoretically easier to address than issues such as long-distance regeneration, reconnection, and neuronal replacement. Such an approach may allow reconstituting a more normal astrocytic environment in the spinal cord, including restoration of extracellular glutamate homeostasis. Astrocyte transport accounts for the vast majority of glutamate removal from the extracellular space, making this an excellent target, despite the over-whelming emphasis placed thus far on modulating synaptic glutamate receptors. Our analysis is consistent with greater numbers of GLT1-expressing cells, as well as greater overall expression, in gray matter areas than in white matter. We also observed different patterns of GLT1 expression changes in gray vs. white matter following SCI. These data suggest the possibility of differential potential for neuroprotection in various regions. Therapeutic strategies could apply to both SCI and traumatic brain injury (TBI), insofar as glutamate and glutamate transporter dysfunction play a role in TBI as well (Yi and Hazell, 2006). Although many key astrocyte functions play a role in the events following SCI and may also be therapeutic targets for treating SCI and other traumatic CNS injuries, the present study focused on one specific and extremely important function of astrocytes, GLT1-based glutamate transport. GLT1 accounts for upward of 90% of CNS glutamate uptake (Maragakis and Rothstein, 2004), suggesting that loss of GLT1 plays a more crucial role than its counterpart, GLAST.

In conclusion, with increased appreciation for the important roles that astrocytes play both in the normal and in the diseased nervous system, this study has focused on temporal and spatial changes in promoter activity regulating expression of one important astrocyte protein, the glutamate transporter GLT1, following SCI. Future work should further elucidate the role of GLT1 and other astrocyte proteins in disease etiology and establish therapeutic targets for the treatment of SCI and other traumatic CNS injuries.

ACKNOWLEDGMENTS

We thank all members of the Maragakis, Rothstein, and Fischer laboratories for discussion. There is no conflict of interest for any author.

Contract grant sponsor: NIH; Contract grant number: F32-NS059155 (to A.C.L.); Contract grant number: NS055976 (to I.F.); Contract grant sponsor: Paralyzed Veterans of America; Contract grant number: 160837 (to A.C.L.).

REFERENCES

Agrawal SK, Fehlings MG. 1997. Role of NMDA and non-NMDA ionotropic glutamate receptors in traumatic spinal cord axonal injury. J Neurosci 17:1055–1063. [PubMed: 8994060]

Baptiste DC, Fehlings MG. 2006. Pharmacological approaches to repair the injured spinal cord. J Neurotrauma 23:318–334. [PubMed: 16629619]

Basso DM, Fisher LC, Anderson AJ, Jakeman LB, McTigue DM, Popovich PG. 2006. Basso Mouse Scale for locomotion detects differences in recovery after spinal cord injury in five common mouse strains. J Neurotrauma 23:635–659. [PubMed: 16689667]

Cao H, Zhang YQ. 2008. Spinal glial activation contributes to pathological pain states. Neurosci Biobehav Rev 32:972–983. [PubMed: 18471878]

Danbolt NC. 2001. Glutamate uptake. Prog Neurobiol 65:1–105. [PubMed: 11369436]

Faulkner JR, Herrmann JE, Woo MJ, Tansey KE, Doan NB, Sofroniew MV. 2004. Reactive astrocytes protect tissue and preserve function after spinal cord injury. J Neurosci 24:2143–2155. [PubMed: 14999065]

Gaviria M, Privat A, d'Arbigny P, Kamenka J, Haton H, Ohanna F. 2000. Neuroprotective effects of a novel NMDA antagonist, Gacyclidine, after experimental contusive spinal cord injury in adult rats. Brain Res 874:200–209. [PubMed: 10960605]

Gincel D, Regan MR, Jin L, Watkins AM, Bergles DE, Rothstein JD. 2007. Analysis of cerebellar Purkinje cells using EAAT4 glutamate transporter promoter reporter in mice generated via bacterial artificial chromosome-mediated transgenesis. Exp Neurol 203:205–212. [PubMed: 17022974]

Grossman SD, Wolfe BB, Yasuda RP, Wrathall JR. 1999. Alterations in AMPA receptor subunit expression after experimental spinal cord contusion injury. J Neurosci 19:5711–5720. [PubMed: 10407012]

Grossman SD, Wolfe BB, Yasuda RP, Wrathall JR. 2000. Changes in NMDA receptor subunit expression in response to contusive spinal cord injury. J Neurochem 75:174–184. [PubMed: 10854260]

Hansson E 2006. Could chronic pain and spread of pain sensation be induced and maintained by glial activation? Acta Physiol 187:321–327.

Holtz A, Gerdin B. 1991. MK 801, an OBS N-methyl-D-aspartate channel blocker, does not improve the functional recovery nor spinal cord blood flow after spinal cord compression in rats. Acta Neurol Scand 84:334–338. [PubMed: 1837648]

Hulsebosch CE. 2008. Gliopathy ensures persistent inflammation and chronic pain after spinal cord injury. Exp Neurol (in press).

Hulsebosch CE, Hains BC, Crown ED, Carlton SM. 2009. Mechanisms of chronic central neuropathic pain after spinal cord injury. Brain Res Rev 60:202–213. [PubMed: 19154757]

Lepore AC, Fischer I. 2005. Lineage-restricted neural precursors survive, migrate, and differentiate following transplantation into the injured adult spinal cord. Exp Neurol 194:230–242. [PubMed: 15899260]

Lepore AC, Han SS, Tyler-Polsz C, Cai J, Rao MS, Fischer I. 2004. Differential fate of multipotent and lineage-restricted neural precursors following transplantation into the adult CNS. Neuron Glia Biol 1:113–126. [PubMed: 16520830]

Lepore AC, Bakshi A, Swanger SA, Rao MS, Fischer I. 2005. Neural precursor cells can be delivered into the injured cervical spinal cord by intrathecal injection at the lumbar cord. Brain Res 1045:206–216. [PubMed: 15910779]

Lepore AC, Neuhuber B, Connors TM, Han SS, Liu Y, Daniels MP, Rao MS, Fischer I. 2006a. Long-term fate of neural precursor cells following transplantation into developing and adult CNS. Neuroscience 139:513–530. [PubMed: 16458439]

Lepore AC, Walczak P, Rao MS, Fischer I, Bulte JW. 2006b. MR imaging of lineage-restricted neural precursors following transplantation into the adult spinal cord. Exp Neurol 201:49–59. [PubMed: 16764862]

Lepore AC, Dejea C, Carmen J, Rauck B, Kerr DA, Sofroniew MV, Maragakis NJ. 2008a. Selective ablation of proliferating astrocytes does not affect disease outcome in either acute or chronic models of motor neuron degeneration. Exp Neurol 211:423–432. [PubMed: 18410928]

Lepore AC, Rauck B, Dejea C, Pardo AC, Rao MS, Rothstein JD, Maragakis NJ. 2008b. Focal transplantation-based astrocyte replacement is neuroprotective in a model of motor neuron disease. Nat Neurosci 11:1294–1301. [PubMed: 18931666]

Li S, Mealing GA, Morley P, Stys PK. 1999. Novel injury mechanism in anoxia and trauma of spinal cord white matter: glutamate release via reverse Na^+-dependent glutamate transport. J Neurosci 19:RC16. [PubMed: 10407058]

Liu D, Thangnipon W, McAdoo DJ. 1991. Excitatory amino acids rise to toxic levels upon impact injury to the rat spinal cord. Brain Res 547:344–348. [PubMed: 1884213]

Liu S, Ruenes GL, Yezierski RP. 1997. NMDA and non-NMDA receptor antagonists protect against excitotoxic injury in the rat spinal cord. Brain Res 756:160–167. [PubMed: 9187327]

Maragakis NJ, Rothstein JD. 2004. Glutamate transporters: animal models to neurologic disease. Neurobiol Dis 15:461–473. [PubMed: 15056453]

McDonald JW, Becker D. 2003. Spinal cord injury: promising interventions and realistic goals. Am J Phys Med Rehabil 82(Suppl 10):S38–S49. [PubMed: 14502038]

Mills CD, Fullwood SD, Hulsebosch CE. 2001. Changes in metabotropic glutamate receptor expression following spinal cord injury. Exp Neurol 170:244–257. [PubMed: 11476590]

Mitsui T, Shumsky JS, Lepore AC, Murray M, Fischer I. 2005. Transplantation of neuronal and glial restricted precursors into contused spinal cord improves bladder and motor functions, decreases thermal hypersensitivity, and modifies intraspinal circuitry. J Neurosci 25:9624–9636. [PubMed: 16237167]

Mu X, Azbill RD, Springer JE. 2002. NBQX treatment improves mitochondrial function and reduces oxidative events after spinal cord injury. J Neurotrauma 19:917–927. [PubMed: 12225652]

Norenberg MD, Smith J, Marcillo A. 2004. The pathology of human spinal cord injury: defining the problems. J Neurotrauma 21:429–440. [PubMed: 15115592]

Olsen ML, Campbell SC, McFerrin MB, Floyd CL, Sontheimer H. 2010. Spinal cord injury causes a wide-spread, persistent loss of Kir4.1 and glutamate transporter 1: benefit of 17 beta-oestradiol treatment. Brain 133:1013–1025. [PubMed: 20375134]

Panter SS, Yum SW, Faden AI. 1990. Alteration in extracellular amino acids after traumatic spinal cord injury. Ann Neurol 27:96–99. [PubMed: 2301932]

Park E, Liu Y, Fehlings MG. 2003. Changes in glial cell white matter AMPA receptor expression after spinal cord injury and relationship to apoptotic cell death. Exp Neurol 182:35–48. [PubMed: 12821375]

Park E, Velumian AA, Fehlings MG. 2004. The role of excitotoxicity in secondary mechanisms of spinal cord injury: a review with an emphasis on the implications for white matter degeneration. J Neurotrauma 21:754–774. [PubMed: 15253803]

Paul C, Samdani AF, Betz RR, Fischer I, Neuhuber B. 2009. Grafting of human bone marrow stromal cells into spinal cord injury: a comparison of delivery methods. Spine 34:328–334. [PubMed: 19182705]

Prow NA, Irani DN. 2008. The inflammatory cytokine, interleukin-1 beta, mediates loss of astroglial glutamate transport and drives excitotoxic motor neuron injury in the spinal cord during acute viral encephalomyelitis. J Neurochem 105:1276–1286. [PubMed: 18194440]

Regan MR, Huang YH, Kim YS, Dykes-Hoberg MI, Jin L, Watkins AM, Bergles DE, Rothstein JD. 2007. Variations in promoter activity reveal a differential expression and physiology of glutamate transporters by glia in the developing and mature CNS. J Neurosci 27:6607–6619. [PubMed: 17581948]

Rosenberg LJ, Teng YD, Wrathall JR. 1999. 2,3-Dihydroxy-6-nitro-7-sulfamoyl-benzo(f)quinoxaline reduces glial loss and acute white matter pathology after experimental spinal cord contusion. J Neurosci 19:464–475. [PubMed: 9870974]

Stys PK. 2004. White matter injury mechanisms. Curr Mol Med 4:113–130. [PubMed: 15032708]

Tanaka K, Watase K, Manabe T, Yamada K, Watanabe M, Takahashi K, Iwama H, Nishikawa T, Ichihara N, Kikuchi T, Okuyama S, Kawashima N, Hori S, Takimoto M, Wada K. 1997. Epilepsy and exacerbation of brain injury in mice lacking the glutamate transporter GLT-1. Science 276:1699–1702. [PubMed: 9180080]

Tao YX, Gu J, Stephens RL Jr. 2005. Role of spinal cord glutamate transporter during normal sensory transmission and pathological pain states. Mol Pain 1:30. [PubMed: 16242033]

Vera-Portocarrero LP, Mills CD, Ye Z, Fullwood SD, McAdoo DJ, Hulsebosch CE, Westlund KN. 2002. Rapid changes in expression of glutamate transporters after spinal cord injury. Brain Res 927:104–110. [PubMed: 11814437]

Watanabe M, Sakurai Y, Ichinose T, Aikawa Y, Kotani M, Itoh K. 2006. Monoclonal antibody Rip specifically recognizes 2′,3′-cyclic nucleotide 3′-phosphodiesterase in oligodendrocytes. J Neurosci Res 84:525–533. [PubMed: 16786579]

Wrathall JR, Choiniere D, Teng YD. 1994. Dose-dependent reduction of tissue loss and functional impairment after spinal cord trauma with the AMPA/kainate antagonist NBQX. J Neurosci 14:6598–6607. [PubMed: 7965063]

Xu GY, Hughes MG, Ye Z, Hulsebosch CE, McAdoo DJ. 2004. Concentrations of glutamate released following spinal cord injury kill oligodendrocytes in the spinal cord. Exp Neurol 187:329–336. [PubMed: 15144859]

Xu GY, Hughes MG, Zhang L, Cain L, McAdoo DJ. 2005. Administration of glutamate into the spinal cord at extracellular concentrations reached post-injury causes functional impairments. Neurosci Lett 384:271–276. [PubMed: 15925447]

Yang Y, Gozen O, Watkins A, Lorenzini I, Lepore A, Gao Y, Vidensky S, Brennan J, Poulsen D, Won Park J, Li Jeon N, Robinson MB, Rothstein JD. 2009. Presynaptic regulation of astroglial excitatory neurotransmitter transporter GLT1. Neuron 61:880–894. [PubMed: 19323997]

Yi JH, Hazell AS. 2006. Excitotoxic mechanisms and the role of astrocytic glutamate transporters in traumatic brain injury. Neurochem Int 48:394–403. [PubMed: 16473439]

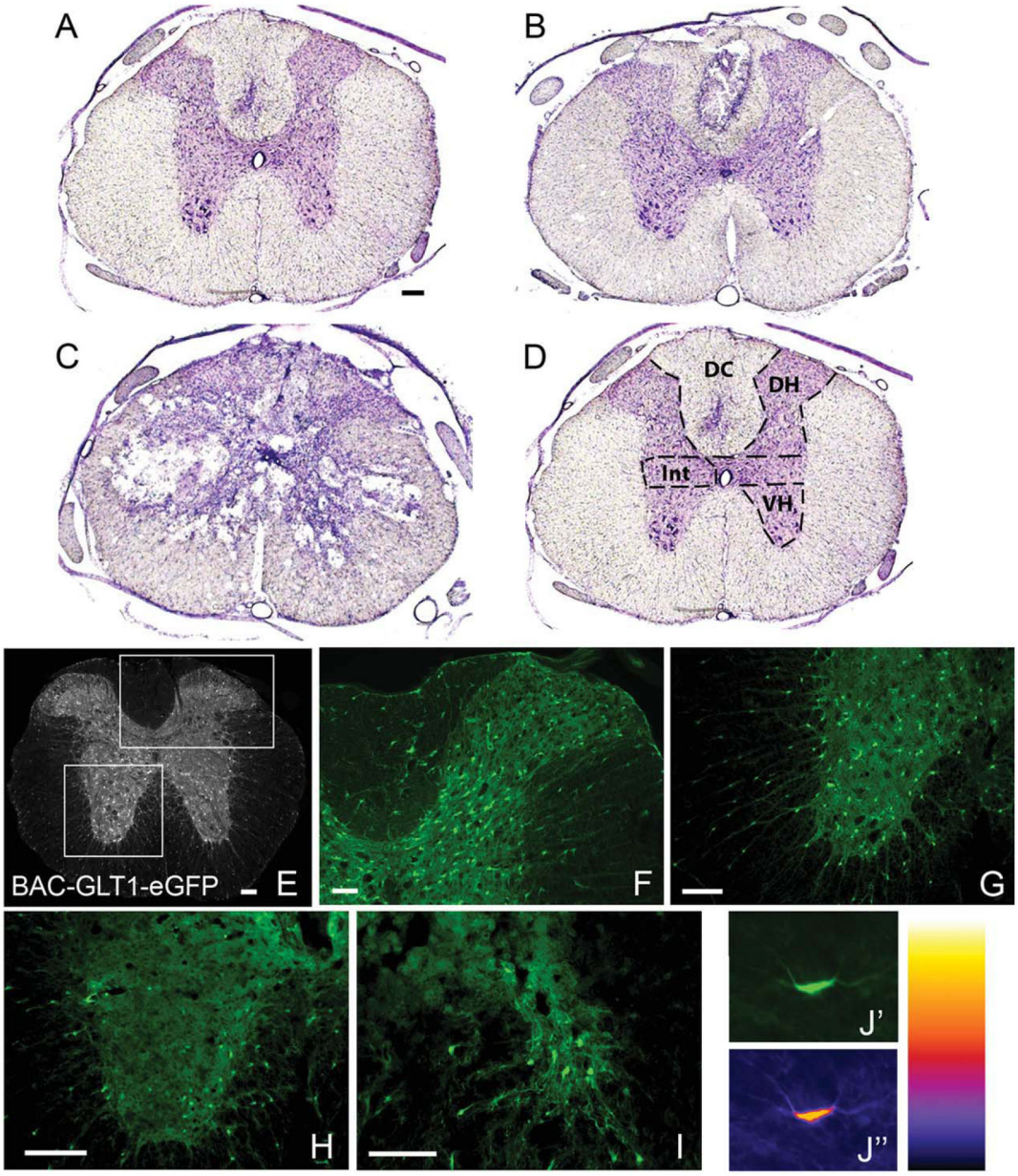

Fig. 1.

Generation of thoracic contusion SCI in BAC-GLT1-eGFP transgenic promoter reporter mice. In cresyl violet-stained sections of thoracic spinal cord from mice that had received a moderate T9 contusion, distinct differences can be observed among intact spinal cord immediately rostral to the injury site (**A**), the rostral periphery of the lesion site (**B**), and the center of the injury (**C**). For BAC-GLT1-eGFP analysis, spinal cord cross-sections were first subdivided into specific anatomical locations (**D**): dorsal column white matter (DC), dorsal horn gray matter (DH), intermediate gray matter (Int), and ventral horn gray matter (VH). In transgenic BAC-GLT1-eGFP reporter mice, GLT1 promoter activity drives expression of the eGFP reporter (E). In normal, uninjured animals (**E–G**), GLT1 is found in abundance in gray matter and to a lesser extent in white matter. To analyze GLT1-eGFP expression in

astrocytes following SCI (examples, rostral intact cord: **H**; epicenter: **I**), individual eGFP$^+$ cells were identified, and the region of fluorescence for each eGFP$^+$ cell was outlined. eGFP average intensity, total intensity, and area for each cell were measured in Metamorph software (**J**). All images are from mice sacrificed at 14 days postsurgery. Scale bars = 50 μm.

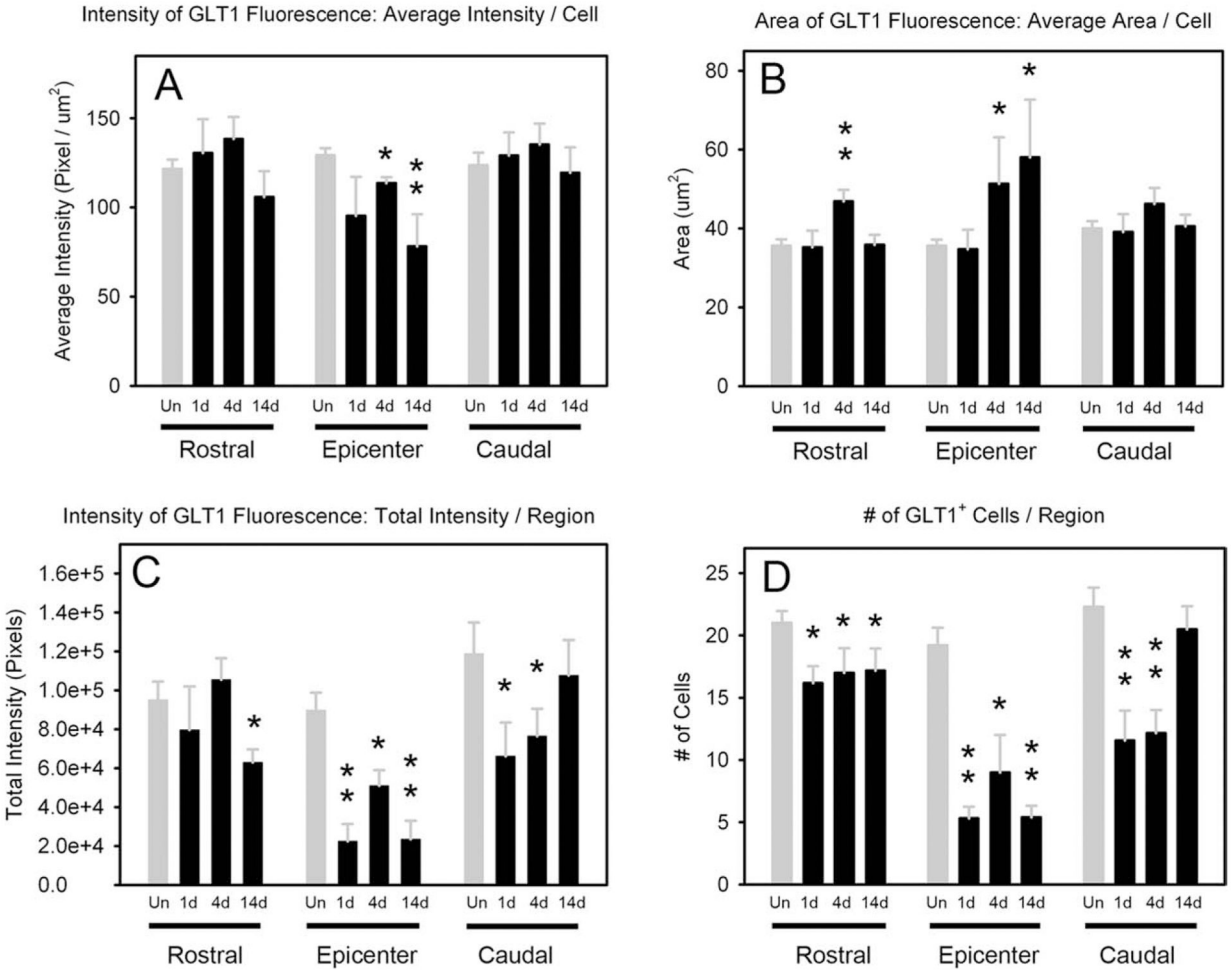

Fig. 2.

GLT1-eGFP expression was reduced in dorsal column white matter astrocytes following thoracic contusion in BAC-GLT1-eGFP mice. At 1, 4, and 14 days post-SCI, BAC-GLT1-eGFP mice were analyzed for average intensity (**A**) and area (**B**) of eGFP expression per cell (defined as cell expressing eGFP) in dorsal column white matter. The total intensity (**C**) of eGFP fluorescence per region (sum of the intensity of all individual eGFP-expressing cells in a region) was analyzed following injury. Total numbers of $eGFP^+$ cells were also counted (**D**). $*P < 0.05$, $**P < 0.001$.

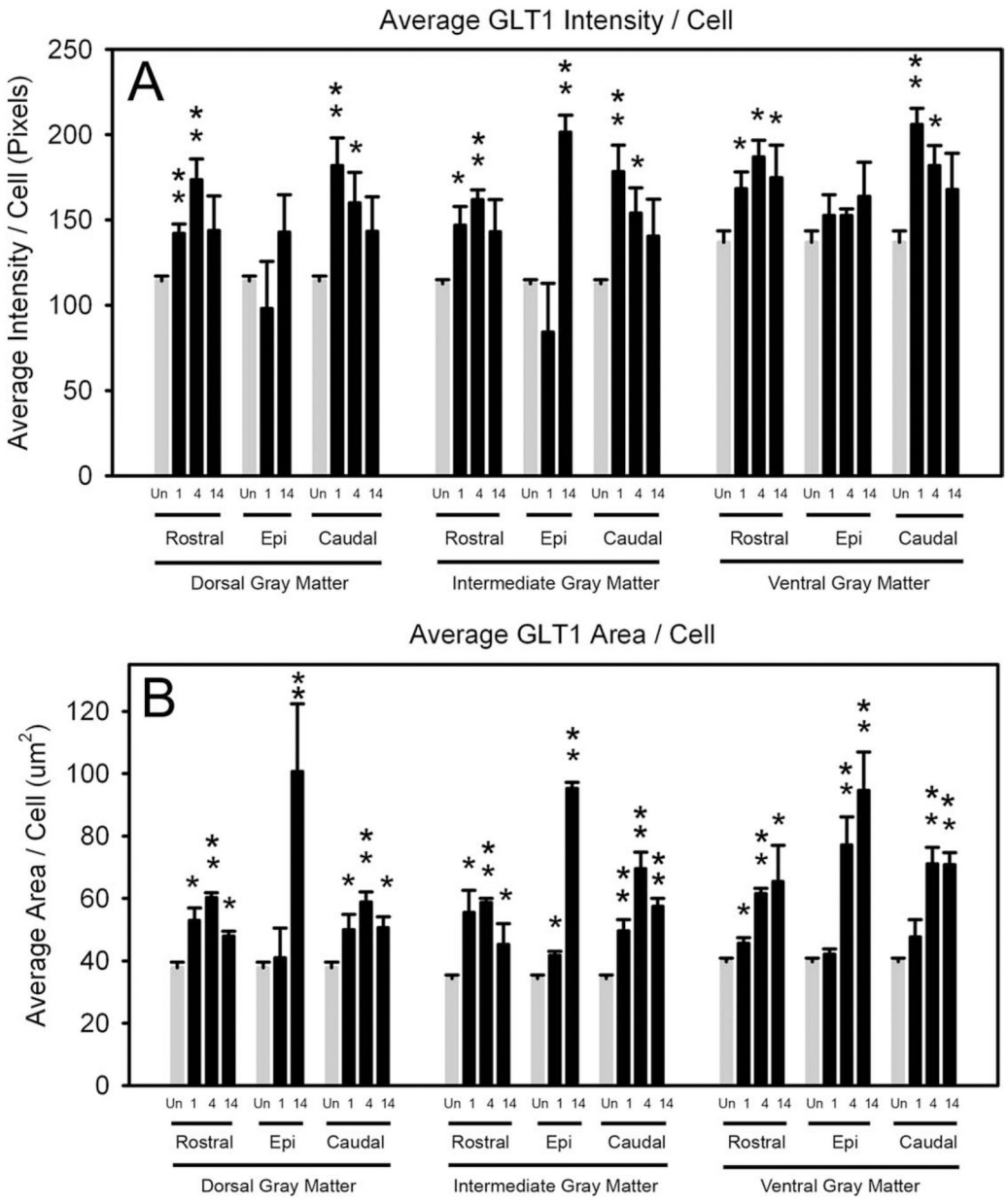

Fig. 3.

GLT1-eGFP expression in individual gray matter astrocytes increased following thoracic contusion in BAC-GLT1-eGFP mice. At 1, 4, and 14 days after thoracic contusion injury, gray matter at the lesion epicenter and in surrounding intact spinal cord was subdivided into dorsal horn, intermediate and ventral horn, as illustrated in Figure 1D. Each gray matter region was analyzed for average individual cell eGFP fluorescence intensity (**A**) and average individual eGFP$^+$ cell area (**B**). *$P < 0.05$, **$P < 0.001$.

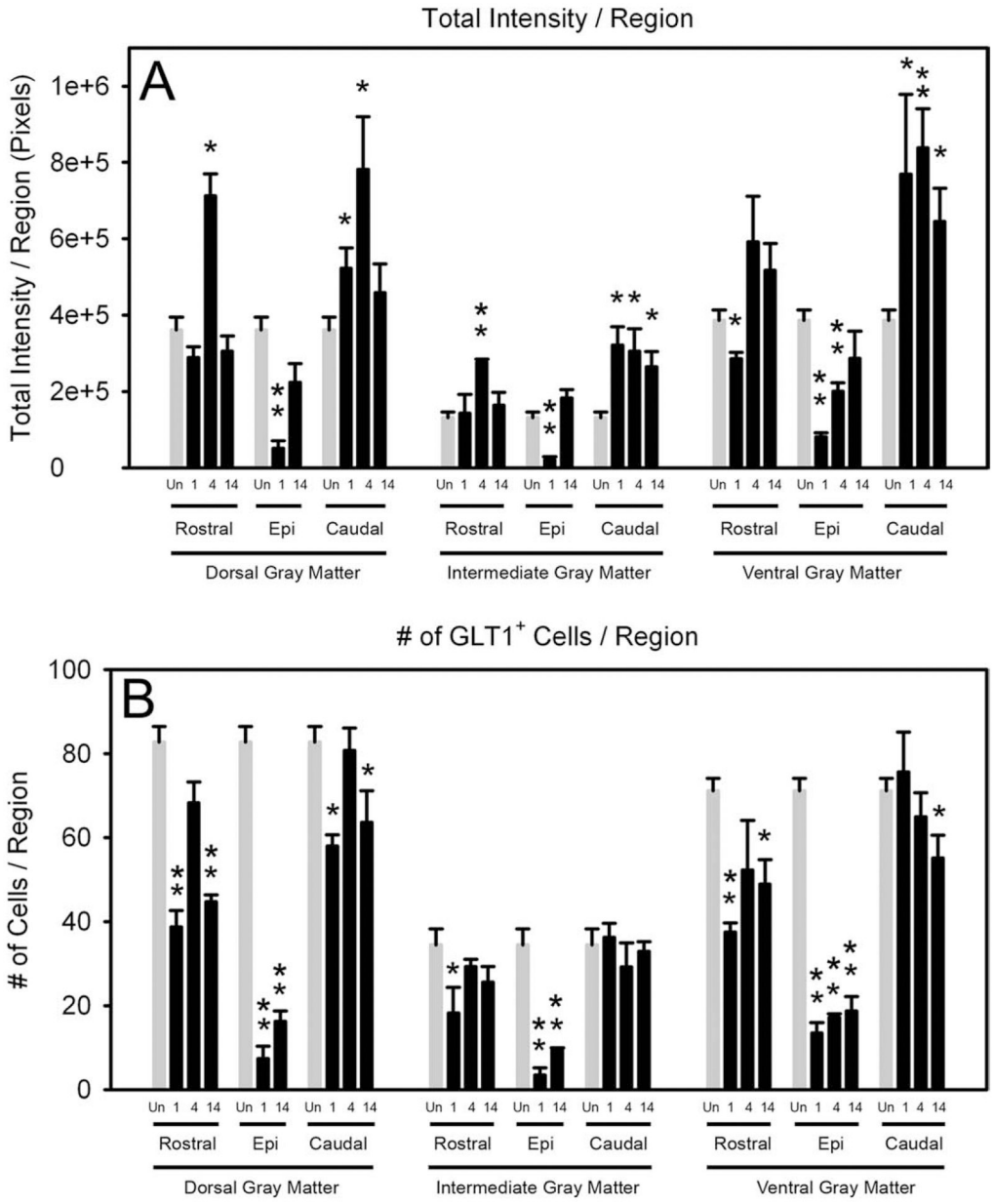

Fig. 4.

Regional GLT1-eGFP expression in gray matter increased following thoracic contusion in BAC-GLT1-eGFP mice. At 1, 4, and 14 days after thoracic contusion injury, each gray matter region was analyzed for combined regional intensities (summation of individual cell intensities of all eGFP$^+$ cells in region; **A**) and counts of eGFP$^+$ cells (**B**). *$P < 0.05$, **$P < 0.001$.

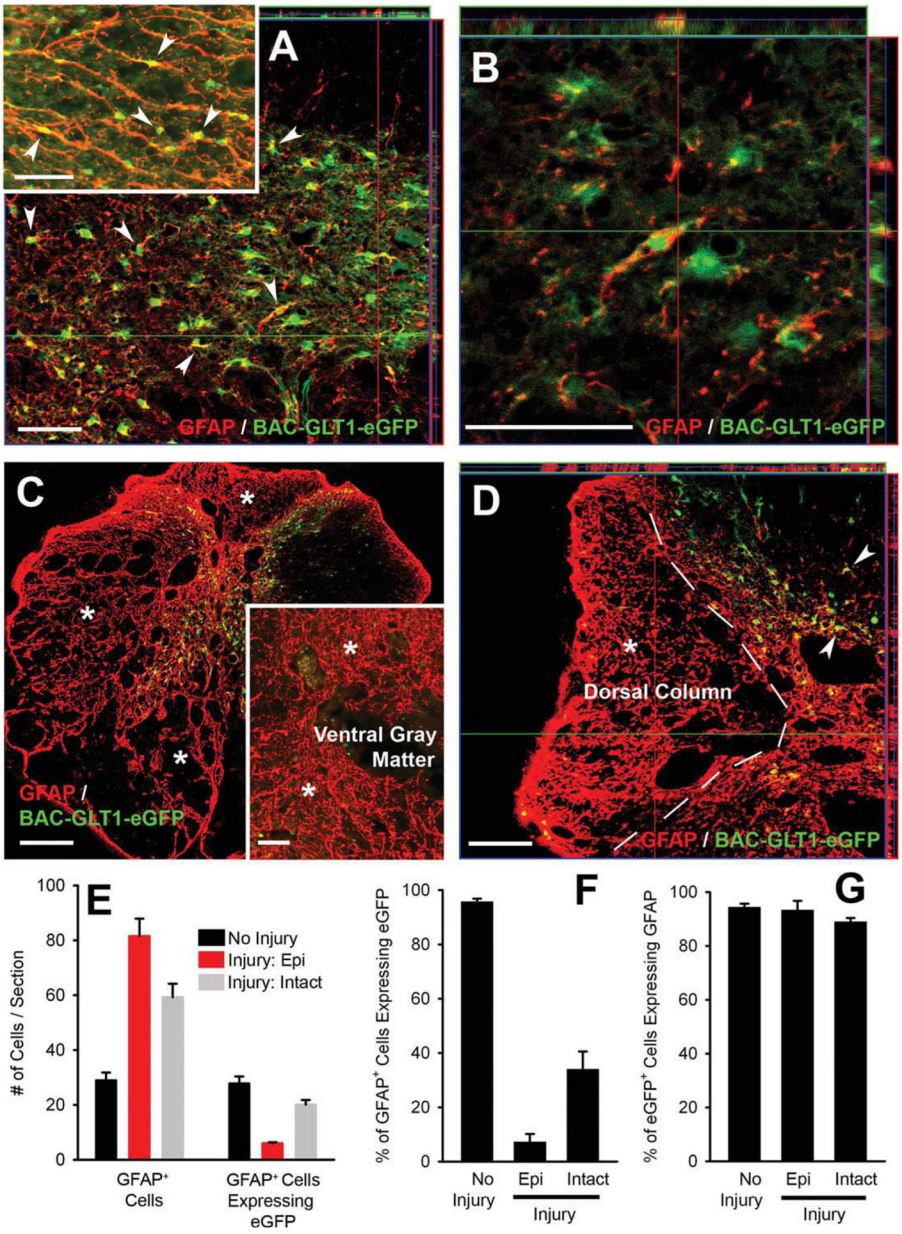

Fig. 5.

GLT1 promoter had limited activity in reactive astrocytes following SCI. In normal uninjured spinal cord, eGFP was expressed only in GFAP$^+$ astrocytes, and nearly all GFAP$^+$ astrocytes expressed eGFP (**A,B**: image from gray matter; **A, inset**: image from white matter, **F,G**). At 4 days following SCI, there was a pronounced increase in GFAP$^+$ astrocytes in dorsal column white matter (**E**), both at the epicenter (**C,D**) and in intact spinal cord immediately adjacent to the epicenter of the injury. However, there was also an overall decrease in numbers of eGFP-expressing cells (see Figs. 2–4). Although eGFP expression was still restricted to GFAP$^+$ astrocytes following SCI (D,G), a large proportion of the increased numbers of GFAP$^+$ astrocytes found at the injury site and adjacent spinal cord did not express eGFP (C,D: white matter; **C, inset**: ventral gray matter, E,F). Areas with large

numbers of eGFP^{-} astrocytes are denoted by asterisks (C,D,C, inset). Arrowheads denote double-labeled cells in A and D. Scale bars = 50 μm.

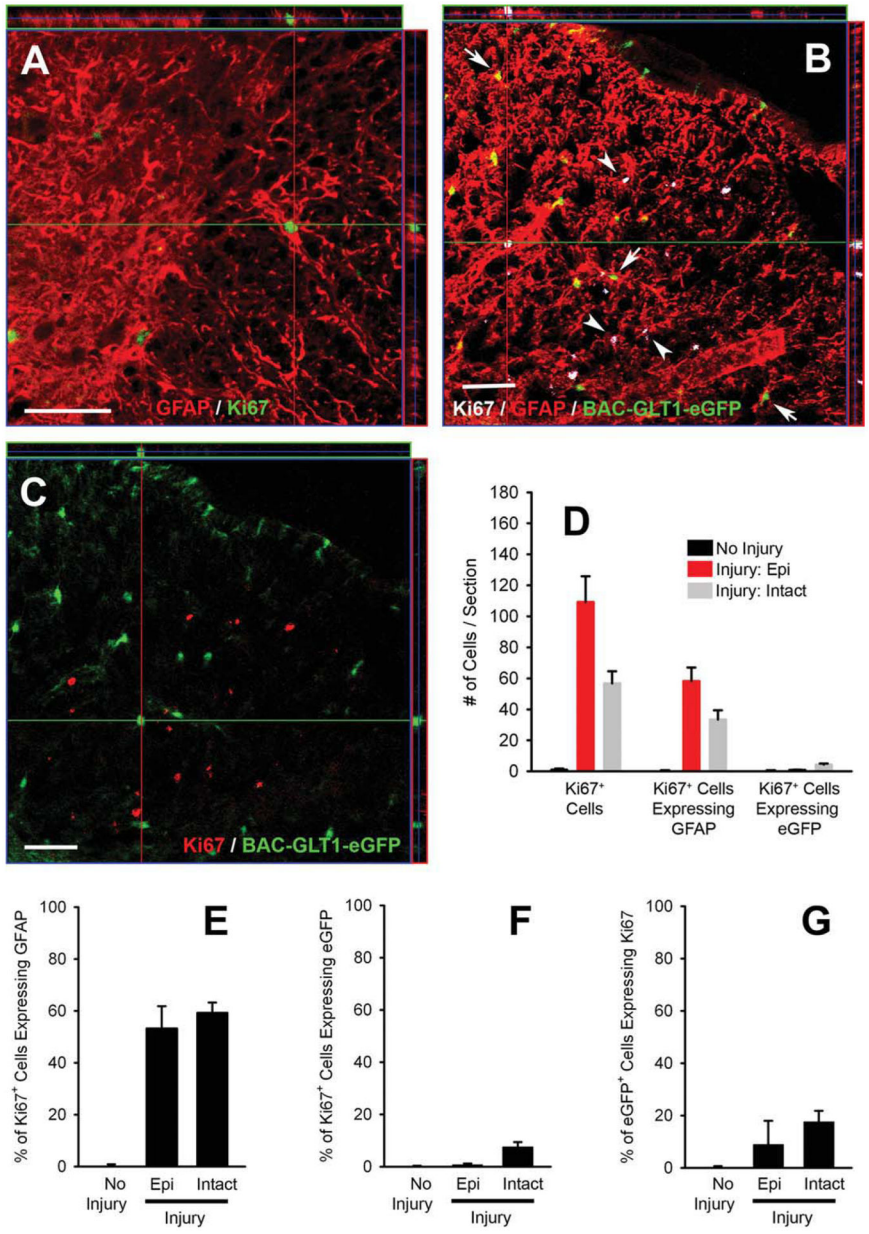

Fig. 6.

Proliferating astrocytes had little GLT1-eGFP expression following SCI. Proliferating Ki67$^+$/GFAP$^+$ astrocytes were observed throughout the lesioned spinal cord (**A,B**). In uninjured spinal cord, few proliferating Ki67$^+$ cells were observed (D). At 4 days following injury, there was a large increase in the numbers of proliferating Ki67$^+$ cells in dorsal column white matter, both at the epicenter and adjacent intact spinal cord (D), and approximately half of the proliferating Ki67$^+$ cells were GFAP$^+$ astrocytes (**D,E**). The vast majority of proliferating astrocytes did not express eGFP (B,**C**,D,**F,G**). Arrowheads denote Ki67$^+$/GFAP$^+$/GLT1-eGFP$^-$ cells. Arrows denote Ki67$^-$/GFAP$^+$/GLT1-eGFP$^+$ cells. Scale bars = 50 μm.

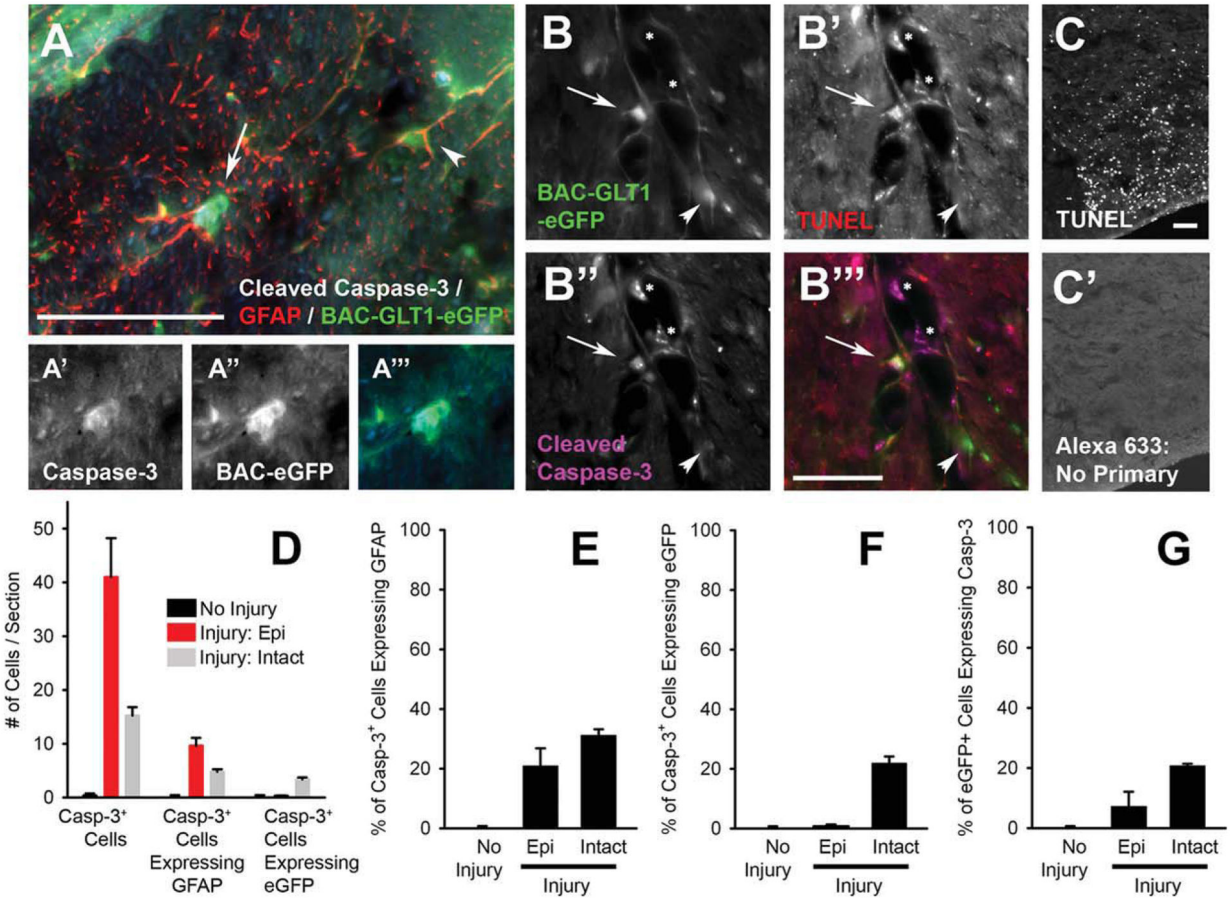

Fig. 7.

GLT1-eGFP expressing astrocytes underwent apoptosis following SCI. Section from injured spinal cord were triple-labeled for the astrocyte marker GFAP, the apoptosis marker cleaved caspase-3, and eGFP (**A**). At 4 days following injury, thoracic spinal cord sections from BAC-GLT1-eGFP mice were also double labeled with cleaved caspase-3 and the apoptotic marker TUNEL (**B**). A control section from injured spinal cord shows positive TUNEL staining (**C**), as well as negative staining for cleaved caspase-3 in the same section when primary antibody for cleaved capsase-3 was omitted (C′). In uninjured spinal cord, rare apoptotic caspase-3^+ cells were observed (D). At 4 days after injury, there was a large increase in the numbers of apoptotic caspase-3^+ cells in dorsal column white matter, both at the epicenter and in adjacent intact spinal cord (D). Approximately 20–30% of the apoptotic caspase-3^+ cells were $GFAP^+$ astrocytes (**D,E**). $GFAP^+$/$eGFP^+$ astrocytes that were caspase-3^+ were noted both at the epicenter (A) and in adjacent intact spinal cord following SCI but constituted only a small portion of the apoptotic cells (D,**F**). Nevertheless, approximately 10–20% of $eGFP^+$ cells at 4 days postinjury in the dorsal column white matter were caspase-3^+ (D,**G**). In A, arrows denote caspase-3^+/$GFAP^+$/GLT1-$eGFP^+$ cells, and arrowheads denote caspase-3^-/$GFAP^+$/GLT1-$eGFP^+$ cells. In B, arrows denote $TUNEL^+$/caspase-3^+/GLT1-$eGFP^+$ cells. Arrowheads denote $TUNEL^-$/caspase-3^-/GLT1-$eGFP^+$ cells, and asterisks denote apoptotic $TUNEL^+$/caspase-3^+ cells that are not GLT1-$eGFP^+$. Scale bars = 50 μm.

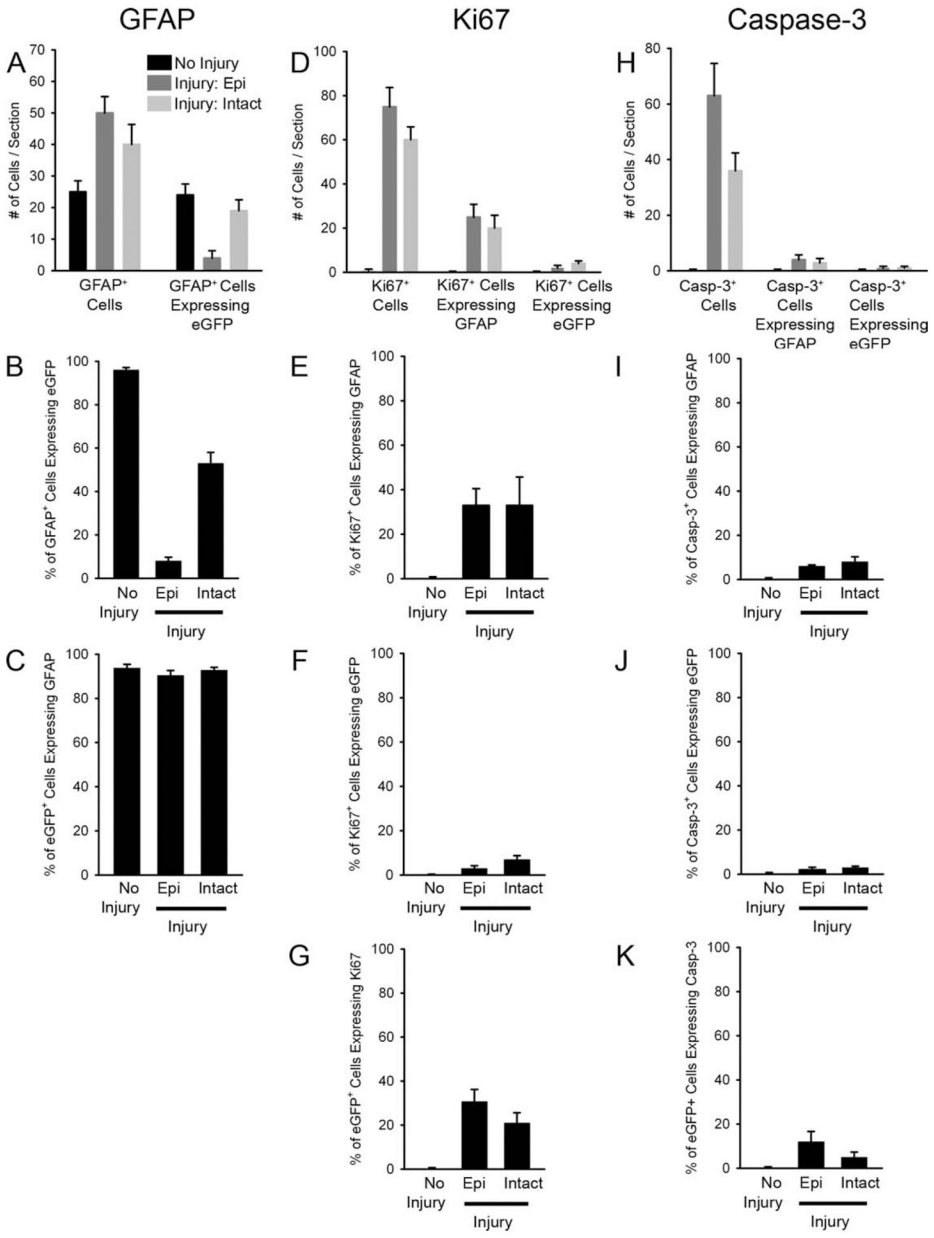

Fig. 8.

Gray matter changes in astrocyte GLT1 expression, proliferation, and apoptosis following SCI. In ventral gray matter at 4 days postinjury, increased numbers of GFAP$^+$ (A) and Ki67$^+$ (D) cells were noted at both contusion epicenter and adjacent intact spinal cord. A large proportion of these additional GFAP$^+$ cells did not express GLT1-eGFP (**A,B**), but GLT1-eGFP expression was still mostly restricted to GFAP$^+$ astrocytes (**C**). Many of the dividing Ki67$^+$ cells were GFAP$^+$ astrocytes (**D,E**), both at contusion epicenter and in adjacent intact spinal cord. Only a small percentage of dividing Ki67$^+$ cells was GLT1-eGFP$^+$ (**F,G**). Finally, a significant increase in apoptotic cleaved caspase-3$^+$ cells was observed following

SCI, both at contusion epicenter and in adjacent intact spinal cord (**H**). A proportion of apoptotic cells was $GFAP^+$ (**I**) and GLT1-eGFP-expressing (**J,K**) astrocytes.

TABLE I.

Antibodies

Antibody	Immunogen	Manufacturer and catalog No.	Dilution	Species and mono-/polyclonal
GFAP	GFAP isolated from cow spinal cord	Dako; No. Z0334	1:400	Rabbit polyclonal
GFAP	Purified GFAP from porcine spinal cord	Millipore; MAB360; clone GA5	1:200	Mouse monoclonal
NeuN	Purified cell nuclei from mouse brain	Millipore; MAB377; clone A60	1:100	Mouse monoclonal
RIP	Rat olfactory bulb	Millipore; MAB1580; Anti-Oligodendrocytes, clone NS-1	1:3,000	Mouse monoclonal
Ki67	Synthetic peptide derived from human Ki67 protein; C-terminus	Thermo; No. RM-9106-S; clone SP6	1:400	Rabbit monoclonal
Cleaved caspase-3	Synthetic peptide corresponding to amino terminus adjacent to Asp175 of human caspase-3	Cell Signaling Technology; No. 9664; Asp175/5A1	1:100	Rabbit monoclonal

TABLE II.

Summary of White and Gray Matter Changes in GLT1-eGFP Expression*

	GLT1-eGFP expression in individual astrocytes	Regional GLT1-eGFP expression	Nos. of GLT1-eGFP-expressing astrocytes
White matter Dorsal column			
Epicenter	↓ Hypertrophy	↓↓↓↓	↓↓↓↓
Intact: rostral/caudal Gray matter Dorsal horn, intermediate area, ventral horn	Minimal changes	↓↓	↓↓↓
Epicenter	↑↑; Moreso at 14 days; very large hypertrophy	↓↓↓ At 1 and 4 day; some recovery by 14 days	↓↓↓↓
Intact: rostral/caudal	↑↑ At all times: not as large at 14 days; hypertrophy	No changes/↑↑ at caudal regions	↓↓↓; Moreso in rostral regions

*All conditions have some exceptions.

TABLE III.

Summary of GLT1-eGFP Expression Changes in Proliferating and Apoptotic Astrocytes

	Astrocyte Nos.	Percentage of astrocytes expressing GLT1-eGFP	Astrocyte division	GLT1-eGFP expression in dividing astrocytes	Astrocyte apoptosis	GLT1-eGFP expression in apoptotic astrocytes
Dorsal column white matter						
No injury	—	~95% GLT1-eGFP only in astrocytes	None	No astrocyte division	None	No astrocyte apoptosis
Epicenter	↑↑↑	~10% GLT1-eGFP only in astrocytes	↑↑↑↑	~10–20% Of dividing astrocytes	~20–30% Of all apoptotic cells	~10–15% Of apoptotic astrocytes
Intact	↑↑	~35% GLT1-eGFP only in astrocytes	↑↑↑	~10–20% Of dividing astrocytes	~20–30% Of all apoptotic cells	~20% Of apoptotic astrocytes
Ventral gray matter						
No injury	—	~95% GLT1-eGFP only in astrocytes	None	No astrocyte division	None	No astrocyte apoptosis
Epicenter	↑↑↑	~10% GLT1-eGFP only in astrocytes	↑↑	~20–30% Of dividing astrocytes	~5–10% Of all apoptotic cells	~10% Of apoptotic astrocytes
Intact	↑↑	~55% GLT1-eGFP only in astrocytes	↑↑	~20–30% Of dividing astrocytes	~5–10% Of all apoptotic cells	~5% Of apoptotic astrocytes